

## Effects of Environment on the Activated Nonradiative Decay of the $^3A_2$ State of $Rh_2(TMB)_4^{2+}$

STEVEN J. MILDER

Received February 6, 1985

The effect of environment on the temperature dependence of the nonradiative decay of the  $^3A_2$  state of  $Rh_2(TMB)_4^{2+}$  (TMB = 2,5-dimethyl-2,5-diisocyanohexane) is studied. The temperature dependence of the observed nonradiative decay rate can be approximately fit to an Arrhenius-like expression:  $k_{\text{obsd}} = k_0 + Ae^{-E_a/RT}$ . Arrhenius parameters are obtained in seven different environments, with the activation energies varying from 1970 to 3420  $\text{cm}^{-1}$ . A plot of  $\ln A$  vs.  $E_a$ , known as a Barclay-Butler plot, is linear, with slope =  $3.3 \times 10^{-3}$  cm and  $y$  intercept = 20.0. The linear Barclay-Butler plot suggests that the activated decay from the  $^3A_2$  state of  $Rh_2(TMB)_4^{2+}$  has the same mechanism, regardless of environment. Single-crystal, dilute-plastic, and dilute-crystal environments have been tested.

### Introduction

The photochemistry and photophysics of dinuclear rhodium(I) complexes have received much attention.<sup>1-6</sup> In particular, complexes with bridging isocyanides have interesting excited-state properties. For example,  $Rh_2b_4^{2+}$  ( $b = 1,3$ -diisocyanopropane) has been shown to both fluoresce and phosphoresce at room temperature in fluid solution, and the phosphorescence is quenched by both energy transfer and electron transfer.<sup>3</sup> The lowest excited state of  $Rh_2(TMB)_4^{2+}$  (TMB = 2,5-dimethyl-2,5-diisocyanohexane) is also a triplet, which can be quenched by both electron transfer and energy transfer.<sup>3</sup> An interesting aspect of the  $Rh_2(TMB)_4^{2+}$  triplet is that its lifetime increases from 10-100 ns at room temperature to 10-25  $\mu\text{s}$  at 77 K. We previously reported the temperature dependence of the emission lifetime of the phosphorescence of this and other dinuclear rhodium(I) isocyanide complexes.<sup>1</sup> The nonradiative decay rates fit an Arrhenius-like expression:  $k_{\text{obsd}} = k_0 + Ae^{-E_a/RT}$ . A slight curvature was seen between the high-temperature and low-temperature limits.

The present work reports the variation of the Arrhenius parameters obtained in the high-temperature limit for  $Rh_2(TMB)_4^{2+}$  in different solvent environments. Though the Arrhenius parameters depend upon the environment, an analysis using the Barclay-Butler correlation<sup>7</sup> strongly suggests that the activated nonradiative decay from the triplet of  $Rh_2(TMB)_4^{2+}$  occurs by the same mechanism regardless of the environment.

### Experimental Section

Luminescence spectra were recorded with a Spex Fluorolog 2 and were corrected for the wavelength response of the instrument. Quantum yields were obtained by the comparison method, with the emission of  $Ru(bpy)_3^{2+}$  used as the standard.<sup>8</sup> Emission lifetimes were taken on an instrument described previously.<sup>3</sup> Briefly, a nitrogen-pumped dye laser (dye = C500,  $\tau = 6$  ns) excites the sample and the emission is collected through a Pacific Precision Instrument 0.45-m monochromator and observed with an EMI D279 photomultiplier. The signal is digitized with a Biomation 6500 transient recorder and transferred to a Z80-based microcomputer for signal averaging and analysis. Variable temperatures were obtained by blowing cooled nitrogen gas at variable rates into a quartz optical Dewar, which held the sample. Temperatures were measured by using a copper-constantan thermocouple. All solution samples

**Table I.** Observed Arrhenius Parameters for the Activated Nonradiative Decay of  $Rh_2(TMB)_4^{2+}$

complex	$E_a$ , $\text{cm}^{-1}$	$10^{-13}A$ , $\text{s}^{-1}$
$[Rh_2(TMB)_4](PF_6)_2$	2980	2
$[Rh_2(TMB)_4](SO_3CF_3)_2$	2630	0.2
$[Rh_2(TMB)_4](BPh_4)_2$	1970	0.02
$Rh_2(TMB)_4^{2+}$ in $H_2O^a$	2660	0.4
$Rh_2(TMB)_4^{2+}$ in $D_2O^a$	2720	0.6
$Rh_2(TMB)_4^{2+}$ in $DMF^a$	2080	0.09
$Rh_2(TMB)_4^{2+}$ in PMMA <sup>b</sup>	3420	3

<sup>a</sup> Microcrystalline sample at low temperatures. <sup>b</sup> Poly(methyl methacrylate) film.

were deoxygenated by either bubbling with Ar gas for 15 min or by four cycles of freeze/pump/thaw degassing. Salts of  $Rh_2(TMB)_4^{2+}$  were prepared by methods previously reported.<sup>2,9</sup>

### Results and Discussion

Figure 1 shows the visible absorption spectrum of  $Rh_2(TMB)_4^{2+}$  when dissolved in EPA' (EPA' = ethyl ether/isopentane/ethanol (5:5:11)) at 295 and 77 K. There is a single band, which has previously been assigned as  $^1A_1 \rightarrow ^1A_2$ ,  $d\sigma^* \rightarrow p\sigma$ .<sup>2,5</sup> As one would expect, it sharpens upon cooling. Excitation into this band gives both fluorescence ( $^1A_2 \rightarrow ^1A_1$ ) and phosphorescence ( $^3A_2 \rightarrow ^1A_1$ ). As can be seen in Figure 2, the fluorescence sharpens and shifts slightly to the blue upon cooling from 295 to 77 K. At 295 K the phosphorescence is so weak it is obscured by the low-energy tail of the fluorescence, while at 77 K the phosphorescence is quite intense. In EPA' the quantum yields are as follows: fluorescence(295 K), 0.021; fluorescence(77 K), 0.030; phosphorescence(77 K), 0.24.

The lifetime of the phosphorescence lengthens upon cooling. As an example, the observed phosphorescence lifetime of crystals of  $[Rh_2(TMB)_4](PF_6)_2$  goes from 80 ns at 293 K to 21  $\mu\text{s}$  at 77 K. We obtained the temperature dependence of the phosphorescence lifetime in a number of environments. Since  $\tau_{\text{obsd}} = 1/(k_{\text{nr}} + k_{\text{r}})$  ( $k_{\text{nr}}$  = the nonradiative decay rate and  $k_{\text{r}}$  = the radiative decay rate), when  $k_{\text{nr}} \gg k_{\text{r}}$ ,  $k_{\text{nr}} = 1/\tau_{\text{obsd}}$ . Plots of  $\log(1/\tau_{\text{obsd}})$  vs.  $1/T$  show low-temperature limits for  $\tau_{\text{obsd}}$  equal to the inverse of the sum of the radiative rate and the temperature-independent portion of the nonradiative rate. At temperatures above 200 K, a linear plot with nonzero slope is found and Arrhenius parameters for the activated nonradiative decay are obtained. An example of one of the Arrhenius plots obtained in the present work is shown in Figure 3. Table I presents the Arrhenius parameters for the activated nonradiative decay for  $Rh_2(TMB)_4^{2+}$  in 7 different environments. The observed activation energy ranges from 1970 to 3420  $\text{cm}^{-1}$ . The large variation in the activation energy might imply that there is more than one temperature-dependent deactivation process occurring and that the relative contributions of

- (1) Rice, S. F.; Milder, S. J.; Gray, H. B.; Goldbeck, R. A.; Kliger, D. S. *Coord. Chem. Rev.* **1982**, *43*, 349.
- (2) Mann, K. R.; Thich, J. A.; Bell, R. A.; Coyle, C. L.; Gray, H. B. *Inorg. Chem.* **1980**, *19*, 2462.
- (3) Milder, S. J.; Goldbeck, R. A.; Kliger, D. S.; Gray, H. B. *J. Am. Chem. Soc.* **1980**, *102*, 6761.
- (4) Miskowski, V. M.; Nobinger, G. L.; Kliger, D. S.; Hammond, G. S.; Lewis, N. S.; Mann, K. R.; Gray, H. B. *J. Am. Chem. Soc.* **1978**, *100*, 485.
- (5) Rice, S. F.; Gray, H. B. *J. Am. Chem. Soc.* **1981**, *103*, 1593.
- (6) Fordyce, W. A.; Crosby, G. A. *J. Am. Chem. Soc.* **1982**, *104*, 985.
- (7) Barclay, I. M.; Butler, J. A. V. *Trans. Faraday Soc.* **1938**, *34*, 445.
- (8) Van Houten, J.; Watts, R. J. *J. Am. Chem. Soc.* **1976**, *98*, 4853.

- (9) Sigal, I. S.; Gray, H. B. *J. Am. Chem. Soc.* **1981**, *103*, 2220.

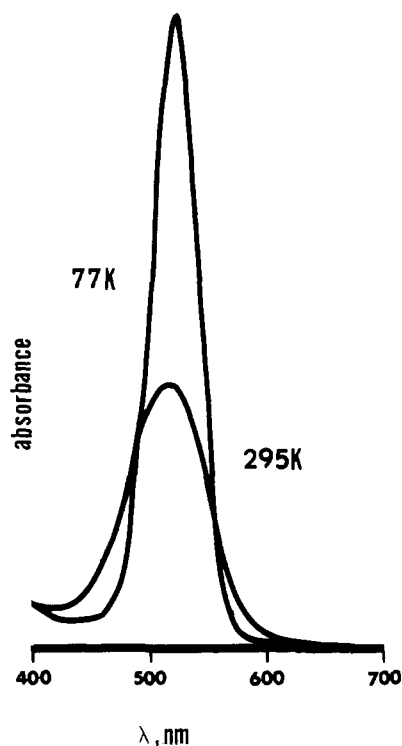


Figure 1. Visible absorption spectrum showing the  ${}^1A_1 \rightarrow {}^1A_2$  ( $d\sigma^* \rightarrow p\sigma$ ) transition of  $Rh_2(TMB)_4^{2+}$  in EPA' at 295 and 77 K.

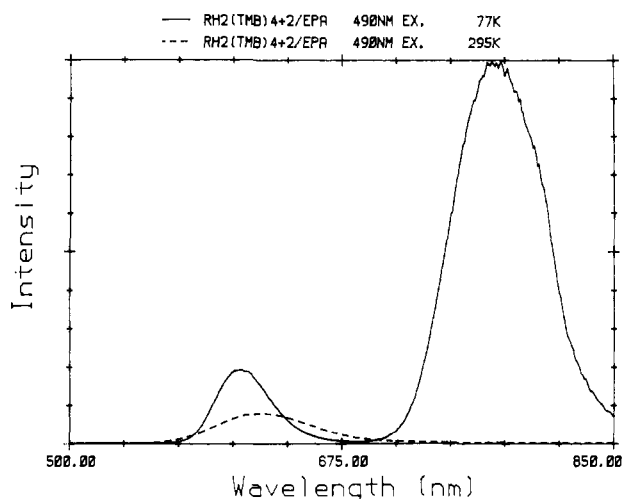


Figure 2. Emission spectrum of  $Rh_2(TMB)_4^{2+}$  in EPA' at 295K (---) and 77K (—). The spectra have been corrected for detector sensitivity.

each mechanism varies with the solvent environment.

One test of whether there is only a single mechanism regardless of the solvent environment is to see if there is any correlation between the Arrhenius parameters obtained for the reaction in different solvents. A linear relationship between  $\ln A$  and  $E_a$  is evidence the reaction has the same mechanism in all of the solvents.<sup>10</sup> The connection between  $\ln A$  and  $E_a$  has been called the Barclay-Butler (BB) correlation.<sup>7</sup> The kinetic parameters in the activated nonradiative decay of the emissive excited states of a number of transition-metal complexes, such as  $Ru(bpy)_3^{2+}$ ,<sup>11</sup> *trans*- $Cr(NH_3)_2(NCS)_4^-$ ,<sup>12</sup> and  $Cr(phen)_3^{3+}$ ,<sup>13</sup> follow the BB correlation. The principle behind the correlation of  $\ln A$  and  $E_a$  is that for a single reaction whose activation energy changes upon changing solvent there is a change in the energy between the

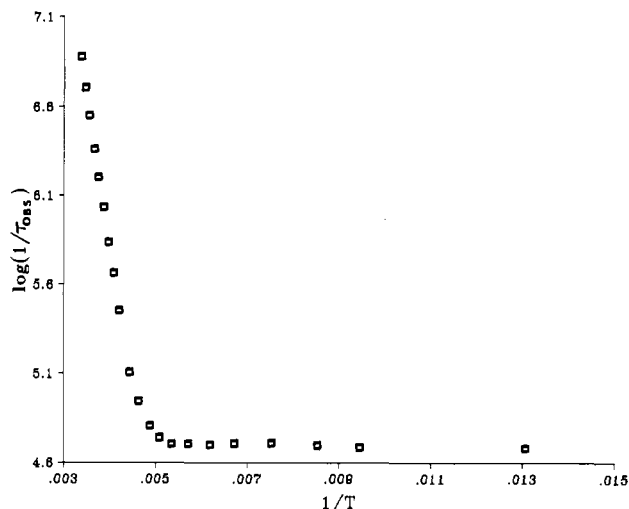


Figure 3. Arrhenius plot of the  ${}^3A_2$  excited-state lifetime of  $[Rh_2(TMB)_4(SO_3CF_3)_2]$ . A linear least-squares fit of the nine highest temperature data points gives  $E_a = 2630 \pm 60 \text{ cm}^{-1}$ ,  $A = (2 \pm 1) \times 10^{12} \text{ s}^{-1}$ , and  $r = 0.999$ .

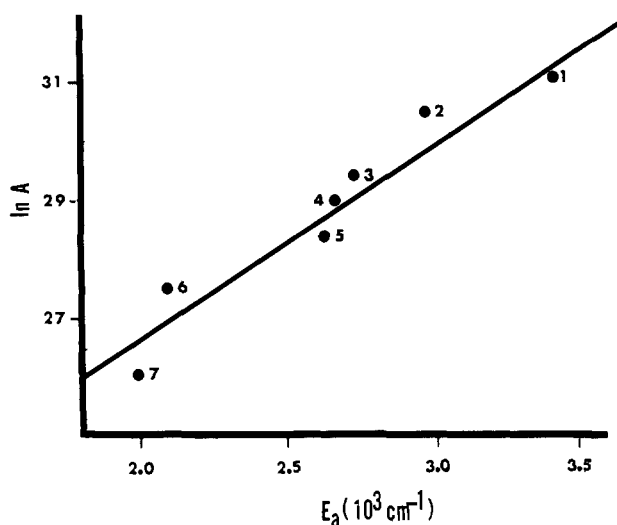


Figure 4. Barclay-Butler plot of the Arrhenius parameters for the activated nonradiative decay of  $Rh_2(TMB)_4^{2+}$ . Slope =  $3.3 \times 10^{-3} \text{ cm}$ ,  $y$  intercept = 20.0, and correlation coefficient = 0.956. Key: 1, PMMA; 2,  $PF_6^-$  salt; 3,  $D_2O$ ; 4,  $H_2O$ ; 5,  $SO_3CF_3^-$  salt; 6, DMF; 7,  $BPh_4^-$  salt.

zero-point energy of the reactant(s) and the transition state. Thus, there should be a correlated change in the density of states at the transition state.<sup>10</sup> A larger activation energy leads to a greater density of states at the transition state, which implies a greater activation entropy and thus a larger preexponential factor.

Figure 4 shows a plot of  $\ln A$  vs.  $E_a$  for  $Rh_2(TMB)_4^{2+}$ . It is linear ( $r = 0.956$ ) with a  $y$  intercept of 20.0 and a slope of  $3.3 \times 10^{-3} \text{ cm}$ . The correlation strongly suggests that the mechanism for the activation of the nonradiative decay does not change upon changing the environment. Thus, the differences in the activation energies are due to the influence environment has on the relative energies of the  ${}^3A_2$  state and the deactivating transition state. Unfortunately, it is difficult to obtain the triplet state energies from absorption measurements, as the  ${}^1A_1 \rightarrow {}^3A_2$  transition is weak. An indirect method for obtaining the difference in the energies of an emissive state in different solvents is to compare the relative energies of the emission maximum. This assumes that the Stokes shift is similar in the solvents. In the present case the triplet emission maximum for  $Rh_2(TMB)_4^{2+}$  at 77 K is shifted  $70 \text{ cm}^{-1}$  to the red in PMMA relative to DMF. It thus appears that the energy of the  ${}^3A_2$  state does not shift nearly as much in energy as  $1340 \text{ cm}^{-1}$ , the difference in the activation energy for the activated nonradiative decay in these two solvents. This implies that changing the solvent strongly affects the position of the

(10) Evans, M. G.; Polyani, M. *Trans. Faraday Soc.* **1936**, *32*, 1332.

(11) Caspar, J. V.; Meyer, T. J. *J. Am. Chem. Soc.* **1983**, *105*, 5583.

(12) Gutierrez, A. R.; Adamson, A. W. *J. Phys. Chem.* **1978**, *82*, 902.

(13) Allsopp, S. R.; Cox, A.; Kemp, T. J.; Reed, W. J.; Sostero, S.; Traverso, O. *J. Chem. Soc., Faraday Trans. 1* **1980**, *76*, 162.

transition state on the reaction coordinates.

In conclusion, the present work strongly suggests that the thermally activated nonradiative decay process is the same for  $\text{Rh}_2(\text{TMB})_4^{2+}$  in all environments tested. As the BB correlation holds in single-crystal, dilute-crystal, and dilute-plastic environments, the deactivation process does not depend on the close proximity of two or more  $\text{Rh}_2(\text{TMB})_4^{2+}$  ions. However, the present work does not imply a mechanism for the deactivation. We have previously postulated that the thermal activation from the  $^3\text{A}_2$  state is possibly to a nonemissive ligand field state.<sup>1</sup> While the current results are not inconsistent with this interpretation, they are by no means conclusive proof. Other reasonable

mechanisms can be envisioned, such as a thermally activated distortion within the  $^3\text{A}_2$  state, which leads to direct crossing to high vibrational levels of the ground state. Further work is in progress on the intimate details of the photophysics of dinuclear d<sup>8</sup>-d<sup>8</sup> metal complexes.

**Acknowledgment.** I thank Drs. Harry B. Gray, David S. Kliger, Robert A. Goldbeck, and Steven F. Rice for helpful discussions during the course of this work. The National Science Foundation (Grants CHE81-20419, PMC83-17044) is acknowledged for partial support of this work.

Registry No.  $\text{Rh}_2(\text{TMB})_4^{2+}$ , 73367-41-6.

Contribution from the Department of Chemistry,  
University of the Witwatersrand, Johannesburg, South Africa

## Anomalous Metal Ion Size Selectivity of Tetraaza Macrocycles

VIVIENNE J. THÖM, GLADYS D. HOSKEN, and ROBERT D. HANCOCK\*

Received September 24, 1984

The apparent paradox that larger metal ions coordinate more strongly to the small macrocycle 12-aneN<sub>4</sub> than to the large 14-aneN<sub>4</sub> is examined. (12-aneN<sub>4</sub> = 1,4,7,10-tetraazacyclododecane; 14-aneN<sub>4</sub> = 1,4,8,11-tetraazacyclotetradecane.) Molecular mechanics calculations (MM) show that, in its trans-I conformer, 12-aneN<sub>4</sub> has a larger cavity, with best-fit M-N lengths of 2.11 Å, compared with 2.05 Å for 14-aneN<sub>4</sub>. In addition, the macrocyclic ring of 12-aneN<sub>4</sub> is more flexible than that of 14-aneN<sub>4</sub>, allowing better response to a change of metal ion size. Thus, as explained by using the MM calculations, most metal ions complex most strongly to 12-aneN<sub>4</sub>, with only small metal ions such as Cu(II) preferring the large 14-aneN<sub>4</sub>. In order to supplement and check existing formation constants on the tetraaza macrocycles, log K<sub>1</sub> values for the following metal ions were determined: with 12-aneN<sub>4</sub>, Cu(II) 23.29; with 13-aneN<sub>4</sub>, Cu(II) 24.36; with 14-aneN<sub>4</sub>, Cu(II) 26.5 (all at 25 °C and in 0.5 M NaNO<sub>3</sub>, determined spectroscopically by using the variation in the UV-visible spectrum as a function of pH); with 13-aneN<sub>4</sub>, Pb(II) 13.48, Cd(II) 12.71; with 14-aneN<sub>4</sub>, Pb(II) 10.83, Cd(II) 11.23 (all determined by glass-electrode potentiometry in 0.1 M NaNO<sub>3</sub> at 25 °C).

Molecular mechanics (MM) calculations have been carried out<sup>1,2</sup> to calculate the hole sizes in tetraaza macrocycles. These calculations have been confined to the case where the metal ion is constrained to lie within the plane of the four nitrogen donors and give best-fit metal to nitrogen bond lengths for these macrocycles as follows:<sup>1</sup> 12-aneN<sub>4</sub>, 1.82 Å; 13-aneN<sub>4</sub>, 1.92 Å; 14-aneN<sub>4</sub>, 2.07 Å; 15-aneN<sub>4</sub>, 2.22 Å; 16-aneN<sub>4</sub>, 2.38 Å. By analogy with the behavior with the crown ethers,<sup>3</sup> if the metal ions were constrained to lie in the plane of the nitrogen donors, we might expect the highest stability in the complexes of metal ions with the member of the above series that most closely fitted the bond length requirements of the metal ion.

Examination of the literature<sup>4</sup> shows that this is not the case. First, a metal ion such as Zn<sup>2+</sup>, which has a best-fit M-N length in the range 2.1-2.2 Å, shows its greatest stability<sup>4</sup> with the very smallest macrocycle, 12-aneN<sub>4</sub>, rather than 14-aneN<sub>4</sub> or 15-aneN<sub>4</sub>, which should fit it more closely if the requirement of planar coordination is adhered to. Interestingly, the relative preference for 12-aneN<sub>4</sub> over the larger members of the series increases as the metal ion becomes larger. This is seen in Figure 3, where Hg<sup>2+</sup> has log K<sub>1</sub> for 12-aneN<sub>4</sub> some 2 orders of magnitude larger than for cyclam. We have extended the data on log K<sub>1</sub>, the formation constant, for the tetraaza macrocycles by using glass-electrode potentiometry, in this work. With the very large Pb<sup>2+</sup> ion, as seen in Figure 3, the preference for 12-aneN<sub>4</sub> becomes even more marked.

When we examined the reported<sup>5</sup> log K<sub>1</sub> values for Cu(II) with the tetraaza macrocycles from 12-aneN<sub>4</sub> through 14-aneN<sub>4</sub>, a rather puzzling feature was the fact that the stability peaked at

13-aneN<sub>4</sub>. The reported<sup>6</sup> values of ΔH and the energy of the d-d transitions peak at the 14-aneN<sub>4</sub> complex, which, with a best-fit M-N length<sup>1,2</sup> of about 2.05 Å, should fit perfectly around Cu(II) with a strain-free Cu-N length<sup>7</sup> of 2.03 Å. It is thus a rather surprising result that the stability should peak at a macrocycle that is too small for Cu(II), particularly as ΔH and the d-d energies do not peak here. The previous<sup>5</sup> study of the 12-aneN<sub>4</sub> through 14-aneN<sub>4</sub> complexes of Cu(II) was carried out polarographically. An alternate, and potentially more reliable method, is to study these systems by following the electronic spectra as a function of pH. This would require an "out-of-cell" study of the kind carried out by Zompa<sup>8</sup> on Ni(II) with the cyclic amine 9-aneN<sub>3</sub>, where the solutions would be allowed to equilibrate in sealed flasks, each corresponding to a single titration point, before the spectra were recorded.

In this paper, then, we report the glass-electrode potentiometric determination of the formation constants of complexes of Pb(II) and Cd(II) with 13-aneN<sub>4</sub> and 14-aneN<sub>4</sub> and the spectroscopic determination of the Cu(II) complex formation constants with these two ligands, plus 12-aneN<sub>4</sub>. A very clear pattern emerges from all these constants plus the existing literature values, namely, that the larger the metal ion, the greater its preference for 12-aneN<sub>4</sub> becomes. We have carried out MM calculations on tetraaza macrocycles,<sup>2,9,10</sup> which have indicated that metal ion size preference exhibited by these ligands varies with conformation. We examine here the question of how the adoption of different conformers can enable the small ligand 12-aneN<sub>4</sub> to complex more effectively with large metal ions.

- Martin, L. Y.; De Hayes, L. J.; Zompa, L. J.; Busch, D. H. *J. Am. Chem. Soc.* **1974**, *96*, 4047.
- Hancock, R. D.; McDougall, G. J. *J. Am. Chem. Soc.* **1980**, *102*, 6551.
- Lamb, J. D.; Izatt, R. M.; Christensen, J. J.; Eatough, D. J. In "Coordination Chemistry of Macrocyclic Compounds"; Melson, G. A., Ed.; Plenum Press: New York, 1979; p 145.
- Kodama, M.; Kimura, E. *J. Chem. Soc., Dalton Trans.* **1977**, 2269.
- Kodama, M.; Kimura, E. *J. Chem. Soc., Dalton Trans.* **1976**, 116, 1720; **1977**, 1473.

- Anichini, A.; Fabbrizzi, L.; Paoletti, P.; Clay, R. M. *J. Chem. Soc., Dalton Trans.* **1978**, 577. Fabbrizzi, L.; Micheloni, M.; Paoletti, P. *J. Chem. Soc., Dalton Trans.* **1979**, 1581.
- Thöm, V. J.; Boeyens, J. C. A.; McDougall, G. J.; Hancock, R. D. *J. Am. Chem. Soc.* **1984**, *106*, 3198.
- Zompa, L. J. *Inorg. Chem.* **1978**, *17*, 2531.
- Thöm, V. J.; Fox, C. C.; Boeyens, J. C. A.; Hancock, R. D. *J. Am. Chem. Soc.* **1984**, *106*, 5947.
- McDougall, G. J.; Hancock, R. D. *J. Chem. Soc., Dalton Trans.* **1980**, 654.